

CZTS synthesis in aqueous media by microwave irradiation

Venkata Alekhya Madiraju¹ · Kshitij Taneja¹ ·
Manoj Kumar¹ · Raghunandan Seelaboyina¹

Received: 21 May 2015 / Accepted: 23 November 2015 / Published online: 1 December 2015
© Springer Science+Business Media New York 2015

Abstract Copper zinc tin sulfide ($\text{Cu}_2\text{ZnSnS}_4$, CZTS), a p-type semiconductor composed of non-toxic earth abundant elements, is a promising material for absorber layer application in thin film solar photovoltaics. The present work describes a relatively faster and reliable microwave irradiation technique to prepare CZTS powder in aqueous media. The CZTS phase of the as-synthesized powder was confirmed by X-ray diffraction and Raman spectroscopy. Optical properties i.e. band gap determined from Tauc plot of the optical absorption spectrum measured by UV–Vis spectroscopy was 1.27 eV, which is suitable for absorbing the solar radiation. The particle morphology studied under SEM and TEM analysis was found to be a 3D flower-like nanostructure formed from 2D layers of CZTS crystals. Further, the most probable mechanism for the formation of CZTS phase is explained.

1 Introduction

Kesterite structured $\text{Cu}_2\text{ZnSn}(\text{S},\text{Se})_4$ (CZTS), a compound formed from earth abundant and non-toxic constituent elements having a high absorption coefficient of 10^4 cm^{-1} and a band gap of 1–1.5 eV, is a promising absorber layer material for thin film photovoltaics (PV) [1]. CZTS nanoparticles when suspended in a suitable solvent along with binders and dispersants make a nano ink which can be used to deposit the absorber layer in thin film solar cells [2]. Several methods to prepare CZTS nanopowders have

been reported in the literature. Hot injection synthesis [3, 4], high temperature arrested precipitation [5, 6], hydrothermal [7–10] and microwave synthesis [11–15] methods have been the most popular ones for CZTS nano powder synthesis.

Hot injection synthesis method, where sulfur/selenium dissolved in oleylamine is injected into the precursor solution made of chlorides and/or acetates of constituent metals, has been worked upon by many to prepare CZTS [3, 4]. Such process is tedious due to the different conditions at which the metal precursors and sulfur be dissolved in the solvent. Also, the oleylamine used in the process acts as a capping agent over the synthesized particles which require further processing to strip oleylamine [16]. The powders also require excessive washing steps after the reaction due to the greasy nature of oleylamine. High temperature arrested precipitation methods [5, 6] have also been reported for CZTS synthesis. Here, triphenyl phosphine oxide (TPO) is used as solvent. But TPO is highly toxic and its subsequent removal from the powders after synthesis process is difficult. Hydrothermal synthesis has also been reported earlier [7–10] but the reaction times have been very long usually reaching 18–24 h making the process tedious and energy intensive.

The reaction times can be drastically reduced if microwave irradiation is used as a heat source during the reaction. Microwaves are an unconventional source of energy to fuel the reactions especially the temperature driven ones. They are shown to have reduced the reaction times dramatically, increase product yields and enhance product purities by reducing unwanted reactions compared to conventional heating methods. These advantages of microwave assisted synthesis process have encouraged many research groups to utilize microwave irradiation for both organic and in-organic synthesis [17–19]. Recently,

✉ Venkata Alekhya Madiraju
alekhya@bhelrmd.co.in

¹ BHEL Corporate Research and Development, Hyderabad, India

microwave synthesis has also been applied to prepare CZTS powders. But the processes used were the ones used in well-known routes to synthesize a material similar to CZTS i.e. CIGS (Copper Indium Gallium Sulfide/Selenide) [20]. Flynn et al. [11] described a microwave synthesis process in which ethylene glycol is used as a solvent. Another approach to microwave synthesis is using oleylamine as a solvent in a single step heating up procedure which has been reported by Wang et al. [12]. In this method, CZTS is prepared by heating the precursors in a focused microwave reactor at 260 °C for 15 min.

Since most of the reported methods have utilized either toxic or industrially incompatible solvents, a more realistic approach to synthesize CZTS could be hydrothermal synthesis using microwave irradiation. The present work aims to leverage the advantages of both microwave and hydrothermal synthesis methods in terms of reduced reaction time and environment friendly solvent respectively. To enhance the propensity of CZTS formation during the reaction, ammonium hydroxide is added to the reaction mixture so that it can help in the formation of water soluble metal ammine complexes, avoiding excessive and sudden precipitation of metal sulfides and holding appreciable amount of metals in the solution. In effect, this paper presents a unique synthesis method which is relatively simple, milder and potentially scalable to prepare CZTS nano powder using microwave irradiation [21]. Further the influence of thiourea concentration on the CZTS formation is investigated.

2 Experimental section

A typical CZTS nanopowder preparation, copper(I) chloride (0.298 g), zinc chloride (0.151 g), tin(II) chloride (0.209 g) and thiourea (0.34 g) were taken in a microwave vessel made of Teflon, along with 30 ml DI water and 10 ml ammonium hydroxide. A Teflon coated magnet stir bar is added to the reaction mixture to achieve uniform heating across its volume. Further, a heating element is added to the reaction mixture to increase the absorption of microwave energy. Finally the tightly closed vessel is exposed to microwave energy. The reaction is carried out at a constant temperature. The reaction temperature is monitored by a fiber optic (FO) temperature sensor inserted in one of the reaction vessels, designated as the control vessel, which is essentially used to control the microwave reaction i.e. temperature and pressure. Since same constituents are present in all the microwave reaction vessels, it is assumed that the temperature and pressure conditions are same throughout all the vessels. Hence, the feedback from the FO sensor present in the control vessel regulates the microwave power delivered during the reaction. Further,

the in situ pressure generated during the reaction is also monitored by a pressure sensor present in the control vessel. The closed nature of the reaction avoids the escape of solvent that could have been possible due to rapid rise in temperature. Additional advantage of closed vessel process is that the reaction can be carried out at a temperature greater than the atmospheric boiling point of the solvent, eliminating the need of high boiling solvents to reach high temperatures. In-addition, significant rate enhancements can be achieved compared to conventional reflux processes [18]. The reaction is carried for a period of 60–90 min and the resultant reacted solution is taken out and the powder from the solution is collected by centrifugation. The obtained sample is labeled Z1. Four other reactions are carried out in a similar fashion by varying the amounts of thiourea to two, three, four and five times the amount used for the reaction in Z1. The samples are labeled Z2, Z3, Z4 and Z5 respectively.

Phase composition and crystal structure of the synthesized CZTS nanopowder was characterized by the X-ray diffraction (XRD) (Philips diffractometer using Cu-K α radiation). Raman analysis for the sample powder is done using Raman spectrophotometer (STR micro-Model STR 150, 532 nm laser). The particle morphology was studied with HRTEM (FEI TECNAI G2) and the distribution of individual elements in the powder was analyzed with energy dispersive X-ray (Zeiss Supra 55 VP, Oxford Instruments). The particle size distribution of the nano powder was determined by Horiba nano particle size analyzer (SZ-100). The band-gap of the powder was measured by UV-Vis-NIR (near-infrared) spectroscopy (Jasco-V670).

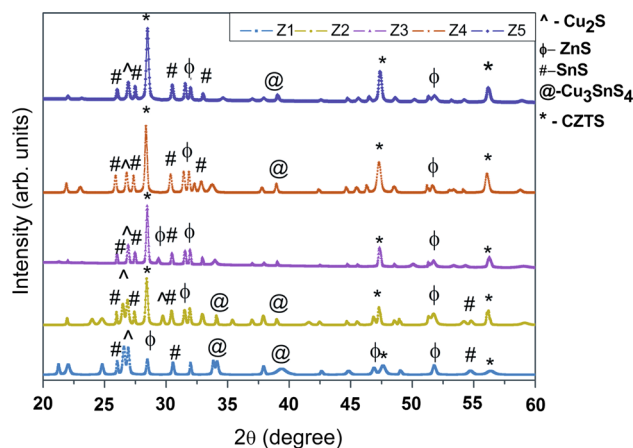


Fig. 1 The XRD pattern of the samples Z1, Z2, Z3, Z4 and Z5. While there is a formation of individual metal sulphides and ternary sulfide at lower thiourea concentrations, the CZTS phase kept improving from Z1 to Z5

3 Results and discussion

Figure 1 shows the XRD image of the synthesized CZTS powder. As seen in the figure, when the reaction was carried out with the required amount of thiourea concentration (represented as Z1) to form $\text{Cu}_2\text{ZnSnS}_4$, many undesired peaks not related to CZTS phase were observed. Closer look at the XRD pattern revealed the other peaks belonged to the sulfides of respective metals i.e. Cu, Zn and Sn. So further reactions, where the precursor concentration was changed as function of thiourea concentration, were carried out. From Fig. 1, which shows the XRD pattern of CZTS powder, it is clear that CZTS phase kept improving as a function of increased thiourea concentration. A closer look at this trend in Fig. 1 reveals two important things. First, individual metal sulfide peaks kept disappearing. Second, the relative intensity of the CZTS as compared to individual metal sulfide peaks enhanced. It can also be observed (Fig. 1) that there is only a slight improvement in the XRD pattern from Z4 to Z5. Therefore, it was established that five times thiourea concentration is optimum to achieve better CZTS phase.

However, the mechanism of CZTS formation as function of thiourea concentration is not completely understood and is the subject of our future work.

To further enhance the purity of the CZTS phase, the reaction time is increased from 60 to 90 min while keeping the precursor concentration as in the sample Z5. Compared to Z5 phase formed for lower reaction time, the 90 min reaction shows improved CZTS peaks (Fig. 2). All the peaks in the XRD pattern of Fig. 2 match well with the peaks in standard JC PDS 26-0575 of CZTS. The major peaks at diffraction angle $2\theta = 28.5^\circ$, 47.33° and 56.17°

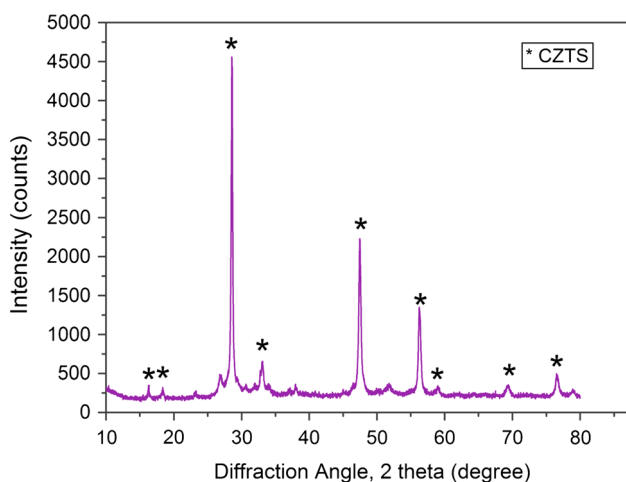


Fig. 2 The X-ray diffraction pattern for 90 min microwave synthesized CZTS. Apart from the major peaks at $2\theta = 28.5$, 47.33 and 56.17 , other minor peaks corresponding the CZTS have also been recorded highlighting the crystallinity of the powder

correspond to (112), (220) and (312) planes of CZTS kesterite structure. Other minor peaks in the XRD pattern also correspond to CZTS.

It is widely accepted that the formed CZTS phase cannot be distinguished from possible binary (ZnS , JCPDS 65-1691) and ternary (Cu_2SnS_3 , JCPDS 27-0198) by-products of the reaction by XRD alone [2]. In this regard, Raman spectroscopy has been used for further confirmation of the CZTS phase (Fig. 3). When Raman analysis was conducted with a 532 nm laser of 2 mW laser intensity, the representative CZTS Raman peak is observed at 331 cm^{-1} which shows a shift from the most reported representative peak at $337\text{--}338\text{ cm}^{-1}$ [1, 2]. However, it has been reported that laser intensity utilized for Raman analysis can also result in peak shift [22]. Hence to record the affect of laser intensity on the Raman spectrum of CZTS, data was collected with various intensities of 0.2, 1 and 2 mW (Fig. 3). It can be clearly observed that higher laser intensities caused the shift of the Raman peak from 331 to 338 cm^{-1} . The slight shift of the peak at higher intensities can be attributed to the optically-induced anti-site defect concentration in CZTS [22].

Otherwise, the peaks located between 331 and 338 cm^{-1} , match with the ones reported in literature for CZTS. The absence of peaks at 275 and 352 cm^{-1} attributable to ZnS and the peaks at 267 , 303 and 365 cm^{-1} attributable to Cu_2SnS_3 confirms the absence of the respective phases [23]. This unambiguously confirms that the formed phase corresponds to CZTS. The inclusion of the various constituent elements of CZTS in the as synthesized powder can also be qualitatively deduced from the EDAX analysis as shown in Fig. 4. It is the elemental mapping of the individual elements in the synthesized CZTS powder which shows that all the elements are uniformly distributed in the

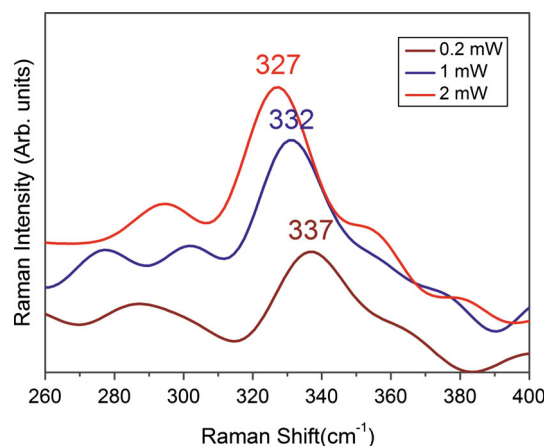


Fig. 3 The A1 vibrational mode of CZTS is shown in the figure. The spectra are recorded at three intensities to understand the effect of intensity of the laser (532 nm) source. The slight shift in the peak at higher intensities may be attributed to the increase of defect sites

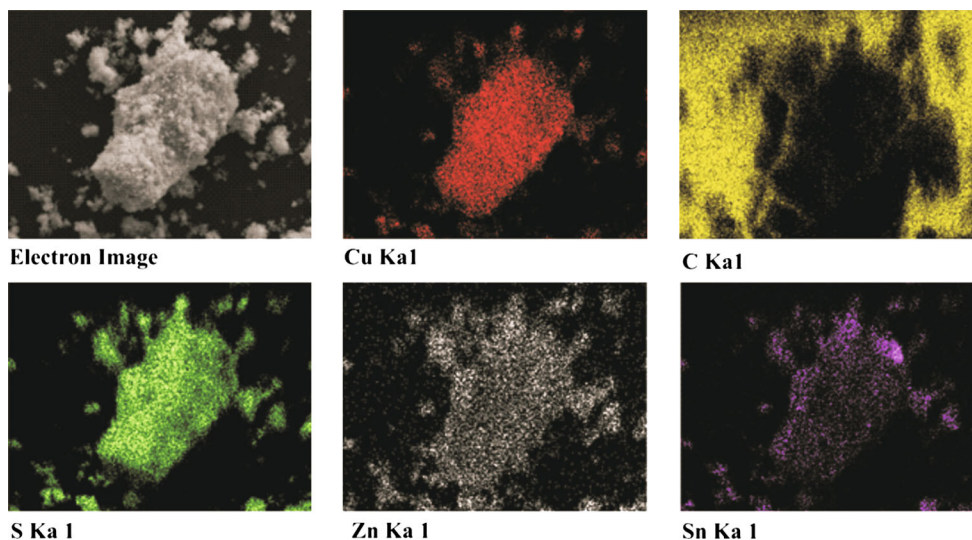


Fig. 4 The elemental distribution of copper, zinc, tin and sulfur is recorded using EDX. The picture qualitatively confirms the uniform distribution of the elements throughout a random particle shown in the electron image

CZTS sample. The EDX shown in the Fig. 4, gives a qualitative picture of the distribution of the individual elements in the sample. The atomic ratios obtained from the EDX detector is 27.51:9.472:10.22:52.74. Clearly, it is nearer to the ideal 25: 12.5: 12.5: 50 for Cu₂ZnSnS₄. The band gap of the material (Fig. 5) is determined from the Tauc plot showing the absorbance versus wavelength of the CZTS powder. For measuring the absorbance spectra, the CZTS powder is dispersed in isopropanol and sonicated for 5–10 min in a cold water bath and the absorbance of the resultant solution was recorded. The optical absorption spectrum of CZTS nanopowder exhibits good absorbance in visible region of solar spectrum, suggesting relatively

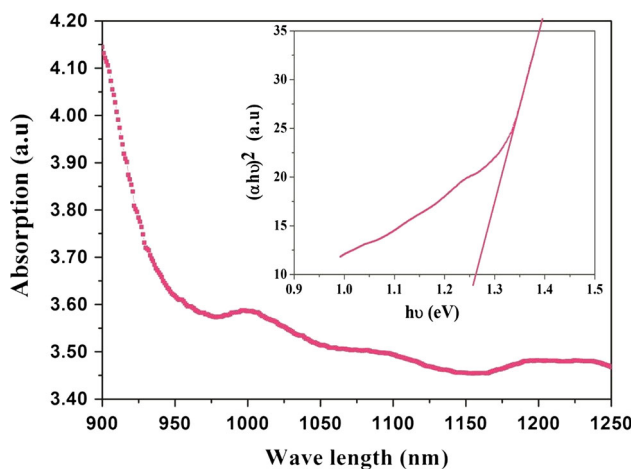
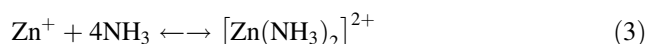
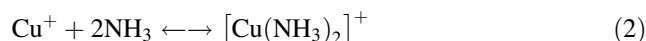
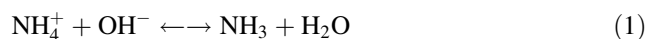


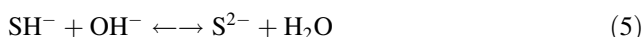
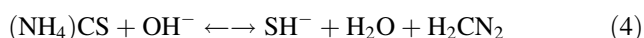
Fig. 5 The absorption spectrum of CZTS powder is recorded and the Tauc plot is drawn with $h\nu$ (eV) on the X axis and $(\alpha h\nu)^2$ on the Y axis (shown in the inset). The powder is dispersed in isopropanol for recording the spectrum

good potential for absorber layer application in thin film solar cells [2]. The measured band gap is determined to be 1.27 eV. The phase stability region for CZTS is smaller as compared to CIGS [24] which might lead to the formation of secondary phases especially ZnS and Cu₂SnS₃ during the reaction. Hence, the band gap tuning is usually done with the incorporation of selenium into the CZTS [2]. Further work in this direction is being done to prepare CZTSSe.

The exact mechanism for the formation of CZTS phase in the present work is not clearly understood. From Fig. 1, it can be concluded that metal sulfides form during the reaction. In the present reaction, it is assumed that there may be two competing processes. One is the tendency of the metals to form soluble ammine complexes and other is the formation of precipitate of metal sulfides. With the right amount of ammonium hydroxide, formation of metal sulfides (usually of slow solubility product) is reduced and metal ions stay in the solution. Based on the experimental observations and the work by Yan et al. [25], the most probable mechanism for CZTS phase is explained as follows. Two of the constituent elements of CZTS namely copper and zinc are transition metals with a large scope for the formation of stable complexes with ammonia. The usage of ammonium hydroxide serves the purpose in two ways. One, it helps in the formation of ammine complexes of Cu⁺ and Zn²⁺ ions present in the solution according to the following equations



These are water soluble complexes which prevent the metal ions of Cu^+ and Zn^{2+} from precipitating out of the solution in the form of hydroxides or sulfides thus, leaving appreciable amount of metals in the solution. But the Sn^{+2} ions present in the solution is not affected by the addition of ammonia and forms a white precipitate of tin hydroxide at room temperature. Nevertheless, the continuous magnetic stirring provided during the reaction keeps the precipitate in contact with the rest of the solution. Second, the hydroxide ion helps in the hydrolysis of the thiourea added to the reaction mixture according to the equations below [26]



As the reaction is started, high instantaneous temperatures are reached due to the rapid transfer of microwave energy to the molecules of the reaction. At these temperatures, it can possibly be expected that the metal-complex ions dissociate to give Cu^+ and Zn^{2+} ions and the tin hydroxide solubility is increased and results in its dissociation to give Sn^{+2} ions into the solution. As the thermodynamic conditions for the formation of CZTS are reached, these metal ions combine with the S^{2-} ion from thiourea to form CZTS. In essence, the in situ availability of all the constituent elements of CZTS along with the instantaneous temperature rise due to rapid and continuous coupling of microwaves is a possible reason for the formation of CZTS as suggested by the X-ray diffraction data shown in Fig. 2. Zhou et al. [27] and Wang [28] provided similar explanations for the growth of CZTS particles.

To determine the particle size distribution, Horiba particle size analyzer which utilizes laser light scattering technique was used. For the sample preparation, a known amount of synthesized powder is dispersed in isopropyl alcohol using sonication. This is done to ensure de-agglomeration of any large lumps of individual particles so that only primary particle size of the powder is detected. Sonication time was varied until the particle size distribution did not change with further increase in sonication time. Also, the concentration of the powder is maintained in such a way that the sample is transparent enough for the laser to reach the detector. The particle size distribution is shown in Fig. 6 where majority of the particles are in the range of 150–600 nm.

The particle size has been correlated with the SEM and the TEM analysis. Figures 7 and 8 depict the SEM and TEM images respectively. From these it can be clearly seen that the morphology of the formed CZTS powder consists of 2D CZTS layers of ~ 5 nm thick and ~ 100 nm length forming a hierarchically 3D flower like structure with irregular shape. The observed structure has been attributed

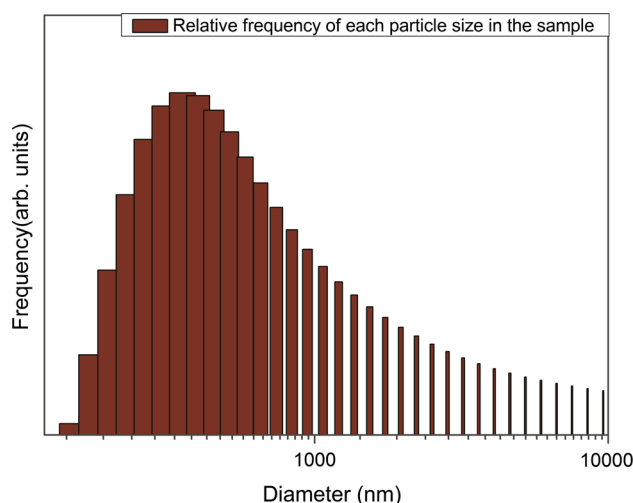


Fig. 6 The particle size distribution of the CZTS powder. It can be seen that most of the particles are between 150 and 600 nm

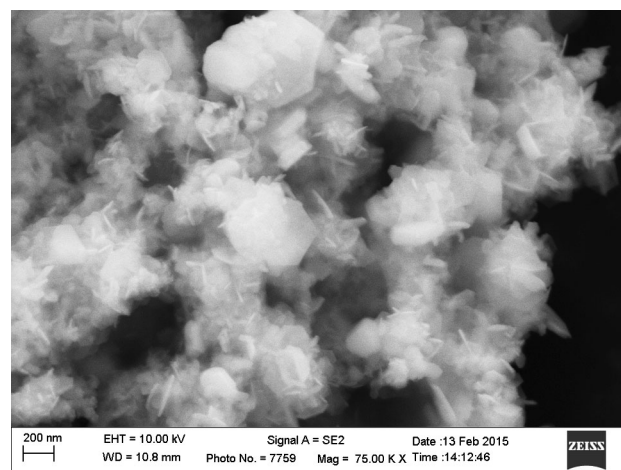


Fig. 7 The SEM image of the synthesized CZTS powder. The particles show irregular growth

to the Ostwald ripening process [10, 27]. Since, the morphology has irregular shape, a broad particle size distribution has been observed. Also, since the particle size analyzer assumes spherical particles when determining the particle size, the distribution shows the majority of the particles in the 150–600 nm range. The larger flower like particles might be more favorable for forming larger grains of 1–2 μm which have been shown to be beneficial for absorber layers with better solar properties [27].

4 Conclusion

A scalable, reliable and environmental friendly synthesis of CZTS powder in aqueous media using a microwave synthesis route has been described. The phase is confirmed by

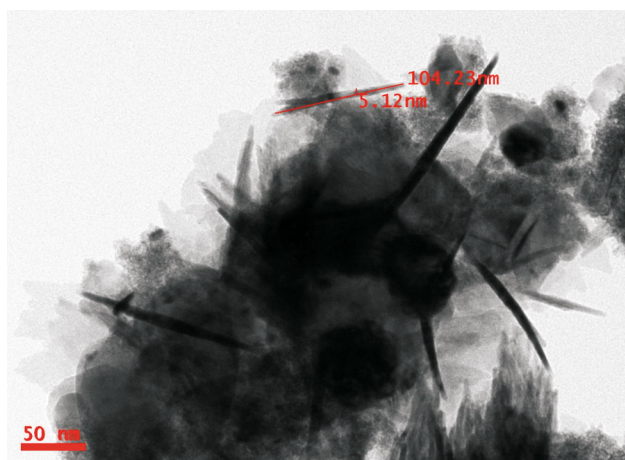


Fig. 8 The TEM image of the synthesized CZTS powder. It is clear from the picture that the morphology is 2D layers of ~ 5 nm thick and ~ 100 nm length

XRD and Raman analysis. Further, elemental mapping using EDX is also presented for a qualitative analysis of the powder. The band gap from UV–Vis spectrum is found to be around 1.27 eV which lies in the ideal range (1–1.5 eV) for absorbing the incoming solar radiation and a TEM analysis revealed a flower like morphology formed from 2D structures of CZTS layers.

Acknowledgments The authors are grateful to Bharat Heavy Electricals Limited (BHEL), Corporate R & D Unit for providing the facilities to carry out the above work. The authors acknowledge the HRTEM facility (FEI TECNAI G2) of University of Hyderabad, Hyderabad, India, Horiba particle size analyzer of Non-Ferrous Materials Technology Development Centre (NFTDC), Hyderabad, India and Raman Spectroscopy facility of International Advanced Research Centre for Powder Metallurgy & New Materials (ARCI), Hyderabad, India.

References

1. D.B. Mitzi, T.K. Todorov, O. Gunawan, M. Yuan, Q. Cao, W. Liu, K.B. Reuter, M. Kuwahara, K. Misumi, A.J. Kellock, S.J. Chey, T. Goislarde de Monsabert, A. Prabhakar, V. Deline, K.E. Fogel, IEEE (2010). doi:10.1109/PVSC.2010.5616865
2. D.B. Mitzi, O. Gunawan, T.K. Todorov, K. Wang, S. Guha, Sol. Energy Mater. Sol. Cells **95**, 1421 (2011)
3. H. Wei, W. Guo, Y. Sun, Z. Yang, Y. Zhang, Mater. Lett. **64**, 1424 (2010)
4. Q. Guo, G.M. Ford, W. Yang, B.C. Walker, E.A. Stach, H.W. Hillhouse, R. Agrawal, J. Am. Chem. Soc. **132**, 17384 (2010)
5. C. Zou, L. Zhang, D. Lin, Y. Yang, Q. Li, X. Xu, X. Chen, S. Huang, CrystEngComm **13**, 3310 (2011)
6. J.Y. Chane-Ching, A. Gillorin, O. Zaberca, A. Balocchib, X. Marieb, Chem. Commun. **47**, 5229 (2011)
7. S. Verma, V. Agrawal, K. Jain, R. Pasricha, S. Chand, J. Nanopart. Res. (2013). doi:10.1155/2013/685836
8. Y. Xia, Z. Chen, Z. Zhang, X. Fang, G. Liang, Nanoscale Res. Lett. **9**, 208 (2014)
9. S.M. Camara, L. Wang, X. Zhang, Nanotechnology **24**, 495401 (2013)
10. V.T. Tiong, J. Bell, H. Wang, Beilstein J. Nanotechnol. **5**, 438 (2014)
11. B. Flynn, W. Wang, C.-H. Chang, G.S. Herman, Phys. Status Solidi A **209**, 2186 (2012)
12. W. Wang, H. Shen, F. Jiang, X. He, Z. Yue, J. Mater. Sci.: Mater. Electron. **24**, 1813 (2013)
13. R. Kaigawa, S. Hirata, M. Sasaki, R. Klenk, Phys. Status Solidi (c) **10**, 1012 (2013)
14. Y. Lin, S. Das, C. Yang, J. Sung, C. Lu, J. Alloy. Compd. **632**, 354 (2015)
15. X. Yang, J. Xu, L. Xi, Y. Yao, Q. Yang, C.Y. Chung, C. Lee, J. Nanopart. Res. **14**, 931 (2012)
16. E.L. Rosen, R. Buonsanti, A. Llordes, A.M. Sawvel, D.J. Milliron, B.A. Helms, Angew. Chem. **123**, 1 (2011)
17. P. Lidstrom, J. Tierney, B. Wathey, J. Westman, Tetrahedron **57**, 9225 (2001)
18. C.O. Kappe, D. Dallinger, S.S. Murphree, *Practical Microwave Synthesis for Organic Chemists: Strategies, Instruments, and Protocols*, 1st edn. (Wiley, Weinheim, 2009), pp. 87–153
19. M. Baghbanzadeh, L. Carbone, P.D. Cozzoli, C.O. Kappe, Microwave-assisted synthesis of colloidal inorganic nanocrystals. Angew. Chem. Int. Ed. **50**, 11312 (2011)
20. R.N. Vora, C. Beall, S. Wei, Y. Yan, M. Romero, G. Teeter, H. Du, B. To, M. Young, R. Noufi, MRS Proc. **1324** (2011). doi:10.1557/opl.2011.844
21. R. Seelaboyina, M. Kumar, A.V. Madiraju, K. Taneja, K. Singh, Curr. Microw. Chem. **1**, 6 (2014)
22. M.Y. Valakh, V.M. Dzhagan, I.S. Babichuk, X. Fontane, A. Perez-Rodriguez, S. Schorr, JETP Lett. **98**, 255 (2011)
23. P.A. Fernandes, P.M.P. Salomé, A.F. da Cunha, J. Alloy. Compd. **28**, 7600 (2011)
24. A. Nagoya, R. Asahi, Phys. Rev. B **81**, 113202 (2010)
25. X. Yan, E. Michael, S. Komarneni, J.R. Brownson, Z. Yan, Ceram. Int. **39**, 4757 (2013)
26. A. Antony, K.V. Murali, R. Manoj, M.K. Jayaraj, Mater. Chem. Phys. **90**, 106 (2005)
27. Y. Zhou, W. Zhou, M. Li, Y. Du, S. Wu, J. Phys. Chem. C **115**, 19632 (2011)
28. W. Wang, H. Shen, X. He, Mater. Res. Bull. **48**, 3140 (2013)